Collagen I-coated titanium surfaces: mesenchymal cell adhesion and *in vivo* evaluation in trabecular bone implants

M. Morra,[1] C. Cassinelli,[1] G. Cascardo,[1] L. Mazzucco,[2] P. Borzini,[2] M. Fini,[3] G. Giavaresi,[3] R. Giardino[3]
[1]Nobil Bio Ricerche, Villafranca d'Asti, Italy

[2]Blood Transfusion Medicine and Biotechnology Laboratory, Santi Antonio e Biagio Hospital, Alessandria, Italy

[3]Experimental Surgery Laboratory, Institute Codivilla Putti, Rizzoli, Orthopaedic Institute, Bologna, Italy

Abstract: The goal of the study was the evaluation of the effect of modification of titanium implants by acrylic acid surface grafting-collagen I coupling. Tests were performed on titanium samples treated by galvanostatic anodization to create a porous surface topography. Surface characterization by X-ray photoelectron spectroscopy (XPS) and scanning electron microscopy (SEM) confirms the biochemical modification of the surface and shows a surface topography characterized by pores mostly below 1 μm diameter. *In vitro* evaluation involving human mesenchymal cells shows enhanced cell growth on collagen coated surfaces as compared to titanium ones. Four weeks *in vivo* evaluation of implants in rabbit femur trabecular bone shows improvements of bone-to-implant contact, while improvement of bone ingrowth is slightly not significant ($p = 0.056$), when compared to the control. Overall, these data indicate that integration in trabecular, or cancellous, bone can be enhanced by the surface collagen layer, confirming previous findings obtained by modification of machined surfaces by the same approach in cortical bone implants. © 2006 Wiley Periodicals, Inc. J Biomed Mater Res 78A: 449–458, 2006

Key words: titanium; surface modification; surface analysis; mesenchymal cells; bone implant

INTRODUCTION

Surface modification of titanium implants for bone contacting applications is presently a very active field of research.[1,2] Ongoing studies are generally aimed at (i) increasing the osteointegration rate (that is increasing the rate of new bone formation) and (ii) addressing issues related to osteointegration in clinically difficult type of bone. This general endeavor is often framed in the widely used slogan: more bone, more quickly. Presently, the most advanced approaches to the surface modification of titanium implant devices involve topography modification,[1,2] the combination of topography and chemico-physical treatments,[3] or the application of inorganic coatings or incorporation of ions.[1,2] As aptly underlined by Hammerle, since topography modification has reached a high level of sophistication, it is expected that significant improvements will occur with the introduction of bio-active coatings, that is with biochemical modification of titanium surfaces.[4] As discussed by Puleo and Nancy, biochemical meth-

ods of surface modification endeavor to use current understanding of the biology and biochemistry of cellular function and differentiation.[5] The goal of biochemical modifications is to immobilize biologically active molecules on device surfaces for the purpose of inducing specific cell and tissue responses.

Among biochemical modifications of titanium surfaces, we have shown that a collagen I coating, covalently linked to a surface-grafted polyacrylic acid layer on titanium implants, can significantly enhance osteointegration rate in a 4 week rabbit model, as evaluated by histomorphometry,[6] bone microhardness measurement,[7] and push-out test.[8] These encouraging results, obtained by biochemical modification of a smooth or, more properly, machined titanium surface, prompted us to evaluate the effects of the same coating on more topographically sophisticated titanium surfaces. The underlying idea is that the optimum implant surface could probably benefit from the synergistic effect of topography and (bio)chemistry. Actually, multifunctional implant surfaces, that is, surfaces that exploit a combination of topography, biochemical cues, and possibly, drug release effects, are a likely avenue of evolution of implant devices.[8,9] Thus, in the present work, the same collagen coating

Correspondence to: M. Morra; e-mail: mmorra@nobilbio.it

was applied to titanium implants surface-treated by galvanostatic anodization.[2,10–12] This technique, presently adopted by a few advanced dental implant systems on the market,[2,13] allows to obtain a surface topography characterized by micron- or nanosize pores, depending on the treatment conditions.[2,10–12]

While previously quoted experiments[6–8] were obtained in cortical bone of rabbit femur diaphyses, the focus of present experiments was trabecular bone. This highly interesting macro-architectural form of bone tissue is of particular relevance for both dental and orthopedic applications of implant devices. Because of its low mechanical properties, trabecular bone is generally defined "poor quality" in clinical settings, despite its obvious biochemical excellence over cortical or "high quality" bone, as described by Davies.[14] Possibly because of the small contribution to primary stability afforded by trabecular bone, the failure rate of dental implants is still higher in the posterior maxilla as compared to other maxillar or mandibular sites where there is more cortical bone. Also, the bony tissue of interest in the growing field of artificial spinal discs, where interfacial bone-device bonding plays an important role, is trabecular in nature.[15]

This article reports the results of a series of experiments aimed at the evaluation of collagen-coated porous titanium surfaces, both in *in vitro* and in *in vivo* implants in trabecular bone. In particular, the aims of this work were the following:

1. The evaluation, in cell-culture experiments, of adhesion and growth of bone-marrow-derived human mesenchymal cells (HMC) to control and collagen-coated samples. Marrow-derived cells play an especially important role in osteointegration in trabecular bone, because the latter has a very high surface area, which is contiguous to the marrow compartment.[14] Marrow that fills the large interconnected pores between the struts and sheets of trabecular bone tissue is the source of HMC. Experiments were performed using HMC in undifferentiated state (as described in the experimental section). In general, studies involving mesenchymal cells and bone contacting devices are performed in media that stimulate osteogenic differentiation[16–18], and much information on the process of new bone formation on implant devices has been gathered by *in vitro* studies in osteogenic media.[19–22] However, in the present work, as discussed later on, the focus is on the initial recruitment of undifferentiated cells to the implant surface. For this reason, and even if this approach has obvious limitations, we preferred to concentrate on the adhesion of undifferentiated HMC. A complete study of the behavior of HMC on the same samples in differentiating VS

control media will be presented in a manuscript in preparation.

2. *In vivo* evaluation of osteointegration by hystomorphometry, using the same 4 weeks rabbit model of previous work.[6–8] This time, however, implants were performed in the trabecular (cancellous) bone tissue of the epiphysis of the distal femurs.

EXPERIMENTAL PROCEDURES

Sample preparation

Galvanostatic anodization of titanium samples

Samples for surface characterization and cell culture studies were obtained from cpTi, grade 2. Samples have a disk shape, the diameter is 8 mm, and the thickness is 2 mm. Fixtures for bone implant studies were obtained from cpTi, grade 2. The fixtures diameter is 1.8 mm and the length 10 mm. Samples were subjected to an anodizing treatment in 0.2% di-sodium hydrogen phosphate (Fluka), dissolved in MilliQ water. The volume of the solution was 200 mL. Anodization was performed in a glass beaker, under stirring; the cathode was a circular titanium sheet covering the beaker wall. The beaker was in turn placed in a big glass flask, filled with water, to control temperature rise upon anodization. Disks or fixtures were placed in the proper sample holders and an anodization was performed in galvanostatic mode up to 230 V. After treatment, samples were extensively rinsed in water and water alcohol solutions and finally subjected to an Ar glow discharge cleaning step. The obtained porosity was analyzed as described in the section on surface characterization. Ti samples anodized as described before will be coded pTi samples.

Collagen coating

Collagen coated anodized Ti surfaces (coded ColpTi) were obtained from pTi samples by the process fully described in Ref. 6. Briefly, in the first step, a polymeric hydrocarbon layer was deposited from propene plasma. Plasma deposition was performed in a capacitively coupled parallel-plate reactor placed inside a class 10,000 clean room. Samples were located on the water-cooled grounded electrode. Both the reactor and the electrodes are made of stainless steel. The reactor volume is about 3 dm^3 and the distance between the electrodes 5 cm. The following treatment conditions were used: 1 min air plasma, 50 W, 20 sccm flow rate (cleaning step), followed by 5 min propylene plasma deposition, 50 W, 100 sccm flow rate (flow rate is controlled by a MKS mass flow controller) (deposition step).

After deposition, treated samples were subjected to acrylic acid grafting. In particular, grafting was performed from a 40% aqueous acrylic acid solution. The solution was gently mixed using a stirrer bar for 2 min. At this point, Argon was

gently bubbled in the solution for 10 min, and then 3% of an acidic solution of ammonium cerium nitrate was added, without discontinuing Ar. The solution was mixed while bubbling for two more minutes, then it was gently poured in test tubes containing the plasma-deposited samples. Grafting was performed for 45 min, at room temperature. At the end of the grafting reaction, samples were rinsed with phosphate buffered saline and MilliQ water (18 MOhm), then stored in water overnight to completely release not surface-linked polymer.

Collagen coupling was performed by immersing the grafted samples in a 0.5% collagen and 1% acetic acid aqueous solution. After 2 h, samples were removed from the solution and rinsed several time in 1% aqueous acetic acid to remove excess adsorbed collagen. After rinsing, samples were immersed in water containing 0.25% EDC and 0.25% NHS, both from Sigma, and kept overnight in this coupling solution. After coupling, all samples were carefully rinsed with 1% aqueous acetic acid, with buffered saline, and finally with MilliQ water and dried under a hood.

Surface characterization

Surface analysis by X-ray photoelectron spectroscopy (XPS)

XPS analysis was performed with a Perkin Elmer PHI 5500 ESCA system. The instrument is equipped with a monochromatic X-ray source (Al Kα anode) operating at 14 kV and 250 W. The diameter of the analyzed spot is ~400 μm, the base pressure 10^{-8} Pa. The angle between the electron analyzer and the sample surface was 45°. Quantification of elements was accomplished using the software and sensitivity factors supplied by the manufacturer.

Scanning electron microscopy and porosity evaluation

Surface morphology of pTi and ColPTi samples was evaluated by scanning electron microscopy (SEM), using a LEO 420 SEM (LEO Electron Microscopy Ltd). The accelerating potential was maintained between 15 and 25 kV, and the relevant instrumental parameters are reported on the micrographs. No preparation was performed on the samples before analysis.

Surface porosity was evaluated by image analysis, using the ImageJ 1.34 software (Wayne Rasband, National Institute of Health, http://rsb.info.nih.gov/ij). Briefly, four random 400×400 pixel fields were obtained from two representative 10k× images from two different samples. Images were filtered using a bandpass filter and thresholded, yielding black pores against a white background. The percent area occupied by the pores, together with the mean pore size, was then measured using the software Analyze Particles routine. Data from pTi and ColpTi samples were compared, and significance of detected differences was evaluated by Student t test.

Cell culture studies

HMC isolation

HMC were obtained from bone marrow samples (10–20 mL) taken from consenting patients undergoing hip replacement surgery. Mononuclear cells were obtained at the interface following Ficoll-Isopaque ($d = 1,077$) sedimentation. Mononuclear cells were plated in T75 Flasks at the density of $2–3 \times 10^5/cm^2$. The cultures were maintained at 37°C in a humidified atmosphere containing 95% air and 5% CO_2. Nonadherent cells were discharged after 48 h. Adherent cells were grown in undifferentiating conditions in Alfa-MEM supplemented with 15% FBS, sodium pyruvate, antibiotic/antimycotic, and glutamine (Invitrogen, San Giuliano Milanese, Italy). Half of the medium was replaced with fresh one every 48 h until subconfluence. At confluence, undifferentiated HMCs were recovered by short trypsine/EDTA (Invitrogen) treatment. An appropriate panel of cluster differentiation antigens (CD14, CD29, CD34, CD44, CD45, CD90, and CD105) was used for flow cytometry analysis of the recovered cells.

HMC culturing

The experimental cell culture medium for HMC consisted of Minimum Eagle's Medium without L-glutamine, 10% fetal bovine serum, streptomycin (100 μg/L), penicillin 1(00 U/mL), and 2 mmol/L L-glutamine in 250-mL plastic culture flask (Corning™). Cells were cultured at 37°C in a humidified incubator equilibrated with 5% CO_2. Cells were harvested prior to confluence by means of a sterile trypsin-EDTA solution (0.5 g/L trypsin, 0.2 g/L EDTA in normal Phosphate Buffered Saline, pH 7.4), resuspended in the experimental cell culture medium, and diluted to 1×10^5 cells/mL.

For experiments, 1 mL of the cell suspension, second passage, was seeded in triplicate for each sample into the 24–well tissue culture polystyrene plates. At selected time intervals, samples were observed by SEM. Briefly, samples were carefully rinsed with PBS and fixed in a 5% glutaraldehyde–PBS. Samples were dehydrated using increasing concentrations of ethanol in water–ethanol solutions up to 100% ethanol. Final dehydration step was performed with hexamethyldisilazane (HMDS, Aldrich). Dehydrated samples were gold sputter-coated (AGAR Auto Sputter Coater) and observed by SEM, using the instrument describe earlier.

Cell counting at fixed time was performed by removing samples from the wells, rinsing with PBS, and placing them in another multiwell plate. Cells were harvested from the samples surface by trypsin and counted in a hemocytometer.

In vivo tests

The *in vivo* study was performed following European and Italian Law on animal experimentation and according to the Animal Welfare Assurance No A5424–01 by the National

Institute of Health (NIH-Rockville, MD). The experimental protocol was sent to the Italian Ministry of Health.

A prehoc power analysis at 80% power, $\alpha = 0.05$, was performed, and it was determined that five rabbits in each group were necessary to detect a change of 40% in the affinity index and bone ingrowth data when comparing CopTi and pTi implants.

Five skeletally mature, adult New Zealand White disease-free rabbits (4.100 ± 0.250 kg) were used. General anesthesia was induced with an i.m. injection of 44 mg/kg ketamine (Ketavet 100, Farmaceutici Gellini SpA, Aprilia Lt, Italy) and 3 mg/kg xylazine (Rompun Bayer AG, Leverkusen, Germany), and assisted ventilation (O_2, 1 L/min; N_2O, 0.4 L/min; isofluorane, 2.5–3%). A 2-cm skin incision was made on the lateral aspect of the distal femoral condyle. Bilateral holes were drilled in both limbs in stages with a 1-mm drill that was subsequently expanded with a 1.8-mm drill. pTi screws were transversally implanted in the right femurs of all rabbits, while ColpTi screws were positioned in the left femurs, up to a total of five implants for each type of screws.

The soft tissues were closed in layers with Dexon 3–0 and silk 3–0. Antibiotic therapy (Cefazolin, 100 mg/kg) was administered preoperatively, immediately after surgery and 24 h later. Analgesics (metamizole chloride, 50 mg/kg) were prescribed in the immediate postoperative period. Four weeks after surgery, the animals were killed by pharmacological euthanasia under general anesthesia, with intravenous administration of Tanax (Hoechst, Frankfurt am Main, Germany).

Femurs were removed, stripped of soft tissues, and prepared for histological and histomorphometric analyses.

Histology and histomorphometry

The femoral condylar trabecular bone containing the implant was fixed in 4% buffered paraformaldehyde for 48 h for undecalcified bone processing. The samples were then dehydrated in graded series of alcohols until the absolute was reached. Finally, they were embedded in epoxy resin (Struers Co. Copenhagen, Denmark). Blocks were sectioned along a plane parallel to the long axis of the implanted screws. A series of sections of 200 ± 10 μm in thickness were obtained with a Leica 1600 diamond saw microtome (Leica SpA, Milan, Italy). Then, sections were thinned to a thickness of 30 ± 10 μm. A total of five trabecular bone implants were analyzed for each material. A total of three sections were analyzed for each specimen by means of histological and histomorphometric studies. They were stained with fast green and acid fucsin and were processed for routine histological and histomorphometric analyses by using a transmission and polarized light Axioskop Microscope (Carl Zeiss GmbH, Jena, Germany) and a computerized image analysis system with Kontron KS 300 software (Kontron Electronic GmbH, Eiching bei Munchen, Germany). After a light microscopy evaluation at various different magnifications, bone histomorphometry measurements were taken semiautomatically by two blinded investigators at a magnification of 12.5×. The following parameters were measured: (1) bone-to-implant contact or affinity index (A.I., the length of bone directly opposed to the implant without the presence of a fibrous membrane/the total length of the bone–implant

interface × 100) and the newly formed bone inside the implanted materials (the bone area/the total implant area × 100). (2) Bone ingrowth, bone area between the screw and the line connecting the thread crests/the total screw thread area × 100

Statistical analysis

Statistical analysis was performed using the SPSS v.12.1 software (SPSS Inc., Chicago, IL). After having verified the normal distribution (Shapiro Wilk test) and the homogeneity of the variance (Levene test), the two-way (surface treatments and experimental times) ANOVA for repeated measures was used to assess significant interactions among selected factors and cell density data. Since histomorphometric results did not present a normal distribution, the nonparametric Wilcoxon signed-rank test, followed by the Monte Carlo methods to compute one-sided probability, was used to highlight significant differences between coated and uncoated screws.

RESULTS

Surface characterization by SEM and XPS

Representative SEM photographs of the samples surfaces are shown in Figure 1. Figure 1(a) (pTi) shows the typical topography obtained by anodization of titanium at high voltage, as widely discussed by Sul and coworkers.[11,23] Pores diameter is, in general, well below 1 μm, as shown in the photograph. Interestingly, no major modification of the surface topography is detected after coating, as shown in Figure 1(b). This result is in general agreement with the nature of the processes used: plasma deposition yields conformal coatings a few nanometer thick[24] and the grafting-coupling process, as discussed elsewhere,[6] involves thickness of the order of 100 nanometer on smooth surfaces. Thus, the nature and overall thickness of the surface-linked layers do not affect the topography imparted by anodization, at least at the hundreds of nm scale. Actually, some indication that the grafted layer could exert a "pore filling" effect was detected here and there, as shown by the 20k× image of Figure 1(c). However, quantitative porosity analysis shows that differences between the two surfaces are not significant, as reported in Table I, both in terms of total porosity and in terms of size of the pores. Quantitative porosity data are in good agreement with those reported by Sul on surfaces obtained using similar treatment conditions,[25] that is porosity is about 25% of the total area. Assuming that pores have a circular shape, which is not always the case, the calculated mean pore diameter is about 350 nm, in good agreement with
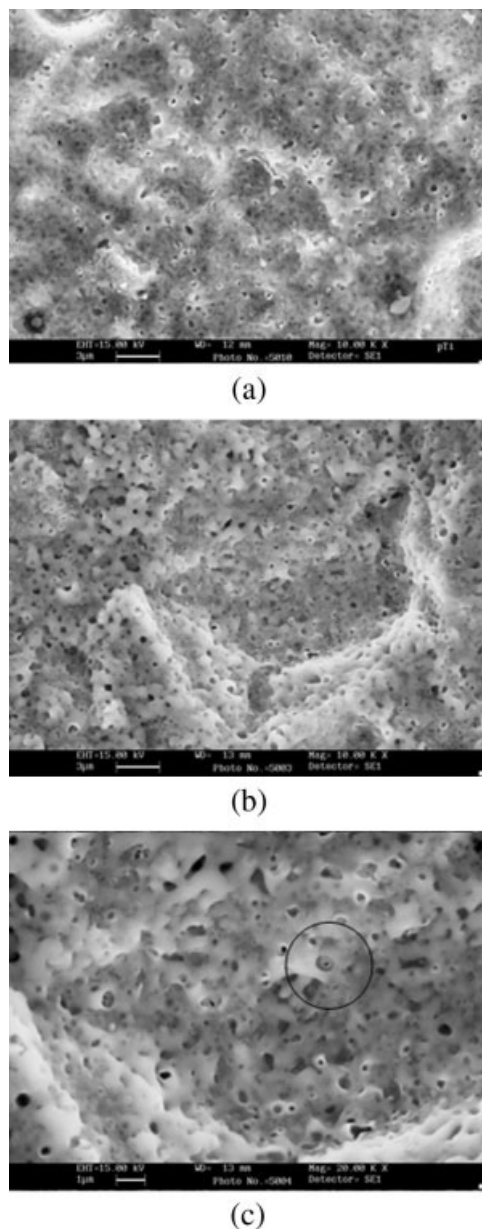
Figure 1. SEM micrographs of (a) pTi, 10k×; b) ColpTi, 10k×; and (c) ColpTi, 20k×. The circle shows a ≈500 nm diameter pore, probably partly filled by the surface grafted layer.

visual inspection of Figure 1 and confirming the correctness of image analysis.

Surface composition of the samples, before and after coating, is shown in Table II. The chemistry detected

TABLE I
Results of Surface Porosity Analysis

	pTi	ColpTi	p
% Porosity	26.4 ± 2.6	24.2 ± 1.1	0.169
Average pore size (μm^2)	0.094 ± 0.009	0.098 ± 0.001	0.593

TABLE II
Surface Composition, as Detected by XPS Analysis, of pTi and ColpTi Samples

Sample	O	C	N	Ti	P	Other (<1%)
pTi	39.1	38.8	0.6	17.3	1.8	Na, Cl, Mg, Si
ColpTi	22.9	59.0	10.9	1.9	3.3	Si, Cl, Na

Value given are expressed in % at.

on pTi is in general agreement with literature data on Ti implant surfaces.[1,2,26] The C/Ti ratio shows a satisfactory degree of surface cleanliness. Phosphorous is incorporated in the surface oxide layer from the anodizing bath, a typical and exploited feature of this kind of approach.[2,24,25]

The ColpTi surface shows a significant amount of nitrogen and an increase in the O/C ratio as compared to pTi. High-resolution C1s peak (not shown) shows a significant contribution of amide (O=C—N) component, and its shape is in general agreement with the C1s peak fully described in our previous work.[7] Overall, surface stoichiometry shows a O/C ratio higher than that found in our previous work on machined titanium surfaces and, contrary to previous findings, some Ti can still be detected.[6,7] Several reasons can account for these findings, and among them, the most likely is related to the rough and peculiar topography of the surface and its interplay with the signal reaching the electron analyzer.[27] In particular, the thickness of the plasma-deposited surface-grafted layer, as well as the photoelectrons yield, is probably significantly different on planar area, walls of the pores, or bottom of the pores. In some of these locations, the surface modified layer can possibly decrease below the XPS sampling depth; moreover, the interplay between slope of the pores and angle of incidence of incoming X-rays complicates the definition of the actual sampling depth. As a consequence, and also because of the comparatively large area probed by XPS, the emitted photoelectrons reaching the electron analyzer bear a convoluted signal from heterogeneous (in the vertical direction) structures, making it difficult to draw direct comparisons with results obtained on relatively smooth machined surfaces. On a general ground, however, the high concentration of nitrogen and the shape of the C1s peak confirm that proteinaceous collagen is indeed on the sample surface, and that bares Ti areas, if any, occupy only a very minor fraction of the surface.

Adhesion and growth of HMC

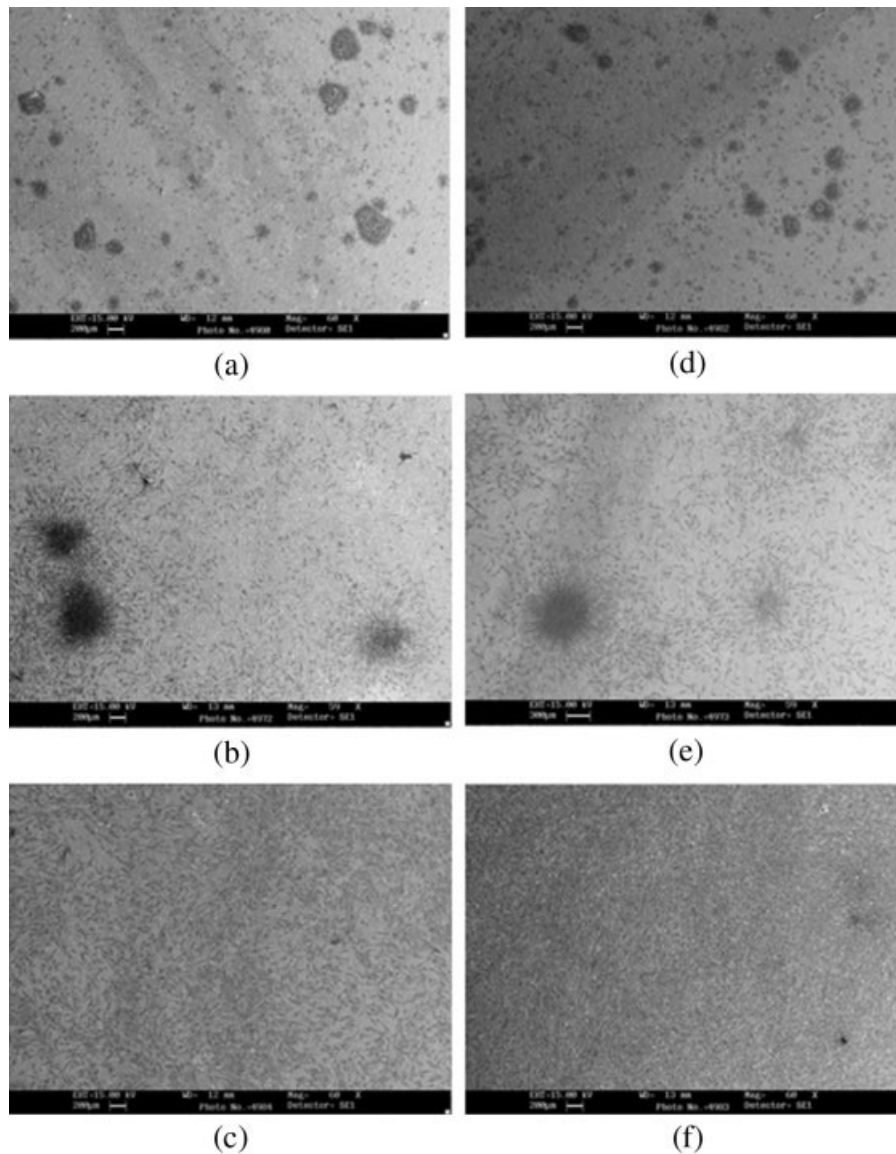Evaluation of adhesion and growth of undifferentiated HMC cells to pTi and ColpTi surfaces, after 2, 24,

Figure 2. Low magnification (60×) images showing the evolution of the process of adhesion and spreading of HMC to pTi (a,b,c) and ColpTi surfaces (d,e,f). Experimental time is 2 h (a,d), 24 h (b,e), and 72 h (c,f).

and 72 h culturing, yields the following information. In general, cells attach to the substrate surface as big aggregates, and then they spread and migrate on the surface. This process is shown in Figure 2, wherein low magnification SEM images at the three different experimental times are collected. At 2 h, a sizable fraction of isolated cells, that is cells not lumped together in big clusters, were still rounded on pTi, as shown in Figure 3(a) (note the relative size of the cell body and the pores). On the other hand, all cells on ColpTi were already spread and flat, with morphology fully conformal to the substrate topography [Fig. 3(b)]. Cell density is higher on ColpTi as compared to pTi, as can be clearly appreciated by the low magnification image of Figure 2 (the fraction of light-colored area, due to the Ti substrate, is bigger in Fig. 2(c) as

compared to Fig. 2(f)), by representative 200× images obtained at 72 h on pTi and ColpTi (Fig. 4; note the exceedingly flat morphology of cells, typical of undifferentiated HMC, that makes imaging of cells very difficult); and by cell counting data (Table III). As to cell morphology, no difference was detected at 72 h, cells were spread and closely following details of surface topography.

Statistical analysis shows a significant interaction of selected factors (surface treatments and experimental times) on cell density results ($F = 49.64$, $p < 0.0005$). Significant increases in cell density results (Table III) are found for ColpTi when compared to pTi at each experimental times ($F = 68.97$, $p < 0.0005$), as well as significant increases between 2 and 72 h within each surface treatments ($F = 76.35$, $p < 0.0005$).
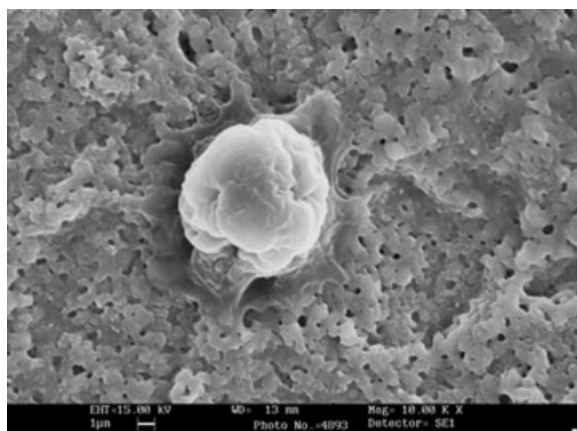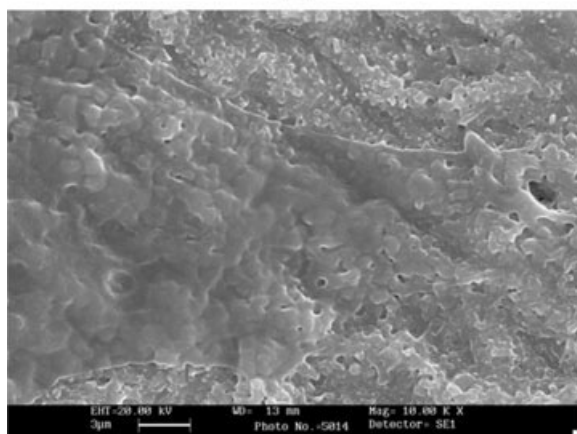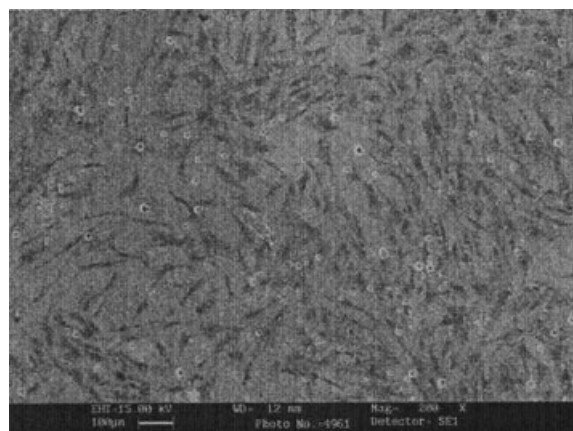
Figure 3. SEM image of HMC on pTi (a) and ColpTi (b) after 2 h culturing.

Figure 4. Representative 200× SEM images of the colonization of pTi (a) and ColpTi (b) by HMC after 72 h culturing.
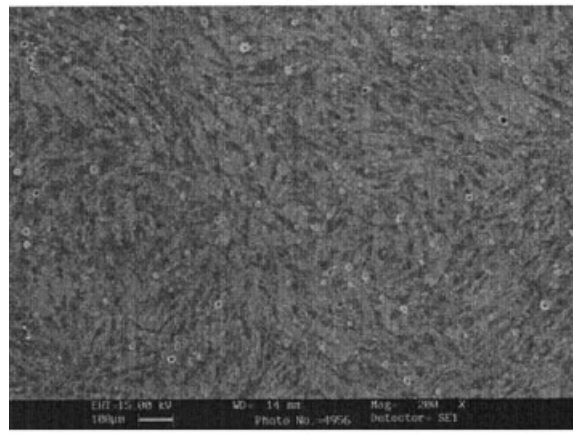
In vivo results

Results of *in vivo* experiments, as obtained by histomorphometry, are reported in Table IV. Figure 5 shows, for each set of samples, a couple of representative photographs of histological sections. At 1 month, mature trabecular bone is grown inside the screw threads in the absence of fibrous tissue at the bone–biomaterial interface in both pTi and ColpTi implants. A higher amount of bone inside the screw threads and in contact with the surface is observed on ColpTi implants [Fig. 5(c and d)].

From a general point of view, both measured parameters are higher on ColpTi samples as compared to pTi, as also suggested by Figure 5. Statistical analysis shows, however, that, while the difference of percent increase of bone-to-implant contact or affinity index is significant at the $p < 0.05$ level ($p = 0.016$), differences between bone ingrowth values are not, albeit marginally ($p = 0.056$).

DISCUSSION

Biomolecular surfaces, obtained by surface-linking of biological molecules that can play an active role in the process of bone regeneration, are a topic of great interest in present day biomaterials and implant devices surface science.[1,2,5] In this work, a collagen I coating, covalently linked to a surface grafted polyacrylic acid layer, was applied to titanium devices. The nature of the surface modification process adopted allows to keep the original surface morphol-

TABLE III
Cell Density (×10⁴ cells/cm²) of HMC Cultures on pTi and ColpTi Surfaces

Time (h)	Material	
	pTi	ColpTi
2	0.89 ± 0.29	1.24 ± 0.27
72	1.37 ± 0.26	5.70 ± 0.85

Values given are in mean ± SD.
$n = 3$, triplicate.

TABLE IV
Histomorphometric Results for Uncoated and Coated
Screws at 4 Weeks

Parameter	Screw	
	pTi	ColpTi
Affinity index (%)		
Median	36.9	63.7*
SEM	4.9	5.5
(Min–Max)	(13.9–42.2)	(38.1–67.7)
Bone ingrowth (%)		
Median	29.0	43.3
SEM	5.7	4.4
(Min–Max)	(11.2–47.2)	(39.7–61.4)

$n = 5$.
Wilcoxon signed rank test: *, $p < 0.05$.

ogy, superimposing biochemical cues to nano-scale topography contribution [Fig. 1, Table I].

Results show enhancement of HMC adhesion and growth (Figs. 2–4) in *in vitro* studies. *In vivo* experiments confirm previous findings obtained in cortical bone implants, using the same approach and animal model.[6–8] Bone ingrowth, in the present case, results marginally nonsignificant as evaluated by statistical analysis, even if raw data suggest a positive trend. Bone-to-implant contact, on the other hand, is significantly improved on ColpTi samples. A mismatch between bone-to-implant contact and bone ingrowth

was also found by other authors while studying different implant surfaces in trabecular bone.[28,29] A strong relationship between bone-to-implant contact and surface properties of the implanted material was detected while bone ingrowth seemed to be also (more) influenced by the healing capacity of the implanted bone.

Considering *in* vivo data, two reflections are required. First, the control sample pTi presents a last-generation surface topography,[10–13] as shown in Figure 1. This topography yields better performances as compared to turned or machined surfaces, as confirmed by a number of literature reports and by clinical practice of commercial implant systems. The observation that further improvement is obtained by the present collagen coating is a clear indication that implant devices can benefit from surface modification processes that combine both conventional topography modification and linking of bioactive molecules.[8] As suggested by Jansen and coworkers, surface roughness effects can be enhanced by other properties such as bioactivity.[30]

The second observation is that improvements obtained by the present collagen coating are, if mean values of the different sets of data are compared, much bigger than those recorded on cortical bone.[6] This is in tune with the nature of the specific bone tissue tested, as described by Davies: trabecular bone is much more biochemically active than cortical bone, and it is prone
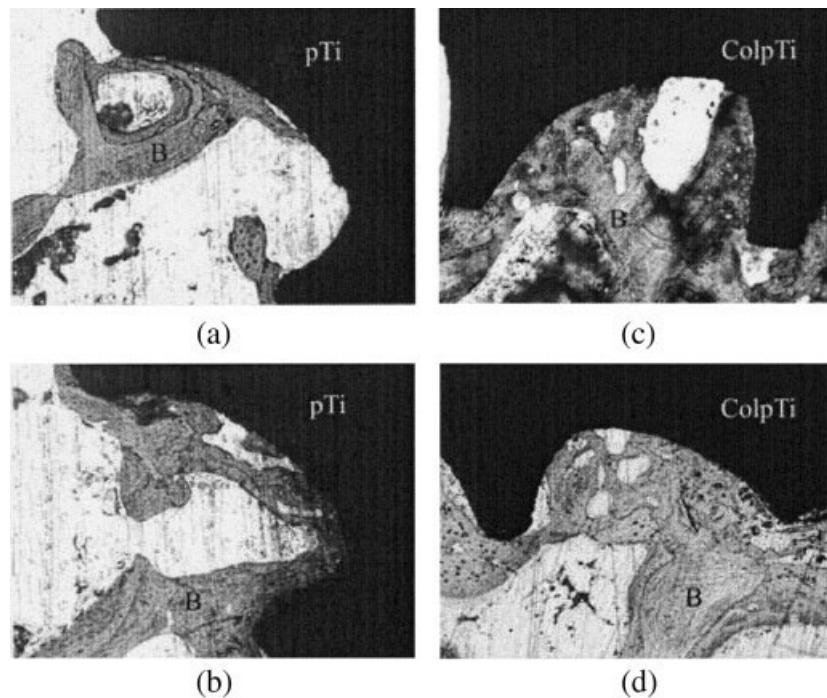

Figure 5. Examples of histological sections obtained from 4 weeks implants in rabbit femur trabecular bone: (a,b) pTi and (c,d) ColpTi. Mature trabecular bone is visible inside the screw threads and reach the implant surfaces without the interposition of fibrous tissue. A higher amount of bone inside the screw threads and in contact with the surface of ColpTi implants is also observable in Figures (c) and (d). (Fast green and acid fucsin, magnification 10×).

to much quicker regeneration and remodeling.[14] Hence, the benefits brought by the implant surface chemistry can be magnified or, in general, accelerated, as compared to cortical bone. From a practical point of view, this is a clear indication of the usefulness of these approaches, since osteointegration in trabecular bone requires fast regeneration of bone tissue in the absence of sufficient cortex to provide stability.

The key question resulting from this and previous work[6–8] is obviously the following: which is the mechanism that improves regeneration of bone tissue at the interface with titanium implants collagen-coated by the present approach? (significant improvement by collagen I coating, with and without the contribution of adhesion peptides, in an *in vivo* model involving implants in foxhounds mandible has recently been reported by Schliephake and coworkers.[31] Also, Kim and coworkers have discussed the stability of collagen coating on titanium in terms of fibrillar assembly, and presented interesting cell response data.[32] However, the surface modification processes used in those papers are completely different from the present one). Several suggestions, taken from the literature, were presented in our previous work. Following Davies arguments,[14] "mineral" approaches, that is speculations based on the possible role of collagen, and of the underlying polyanionic polyacrylic acid layer, as a matrix that can promote calcium binding and quick mineralization should be discarded ("bone formation is initiated by osteoblasts, not the material surface."[33]). *De novo* bone formation on implant surfaces requires, first of all, the deposition of a cementum line, that is, a collagen-free organic matrix secreted by differentiating osteogenic cells. This matrix provides nucleation sites for calcium phosphate mineralization, and it contains two non-collagenous bone proteins, osteopontin and bone sialoprotein, and two proteoglycans, but no collagen. According to Davies, the most critical issue in *de novo* bone formation is the recruitment of osteogenic cells and their migration to the implant surface.[1,14] The formation of bone on biomaterials relies on the presence of undifferentiated mesenchymal cells with the ability to proliferate along the osteogenic pathway. In this respect, the surface layer of collagen of the present study shows a significant advantage, over the pTi surface, in terms of HMC adhesion and growth, as shown in Figures 2–4, albeit with all the limitations of the *in vitro* environment and of the model chosen (undifferentiating medium). Interestingly, our previous experiments using the same coating and continuous Sa-Os2 osteoblast-like cells showed a different trend[6]: the untreated Ti surface yielded a higher cell growth. Collagen, and the cell-binding domains it contains, play an important role in osteoblast cells behavior,[34] promoting osteoblastic differentiation of bone marrow cells and controlling a number of aspects of their progression along the os-

teogenic pathway[35]; collagen integrin receptors regulate early osteoblast differentiation induced by BMP-2.[36] A "strong and rapid (30 min) adhesive interaction" between HMC and collagen I has been described by Salasznyik and coworkers,[37] in agreement with our findings on ColpTi. In the same article,[37] it is reported that adhesion to collagen I promotes differentiation of HMC. On the basis of existing literature, it is then possible to speculate that the ColpTi surface can either or both recruit more osteogenic cells precursors and provide a more favorable environment for osteogenic cells differentiation, following instructions from cell-matrix interactions and from diffusible molecules as compared to the pTi surface (or, more properly, to the surface made up by the protein layer adsorbed from the implant environment to the pTi surface). Always following Davies arguments,[14] the pro-coagulant activity of collagen could also play a significant role through enhanced platelet activation and concurring release of growth factors and, as a consequence, in providing the temporary fibrin-fibronectin-coagulation Factor XIII network matrix required for cell migration to the implant surface.[38] Ongoing dedicated studies are aimed at clarifying this point.

CONCLUSIONS

In conclusion, results of the present work show that it is possible to obtain porous titanium surfaces, with pore diameter in the sub-micron range, bearing a layer of type I collagen linked to a surface grafted polyacrilyc acid layer. Surfaces obtained in this way maintain the porous topography but show enhanced HMC cell adhesion and increased osteointegration properties in trabecular bone, in a four weeks rabbit model, over the pristine titanium surface. These results are a further indication, in the wake of the growing literature on the subject, of the role that biochemical surface modification can play in the development of improved dental and orthopedic implant devices.

References

1. Davies JE, editor. Bone Engineering. Toronto: Em Squared; 2000.
2. Brunette DM, Tengvall P, Textor M, Thomsen P, editors. Titanium in Medicine. Berlin: Springer; 2001.
3. Buser D, Broggini N, Wieland M, Schenk RK, Denzer AJ, Cochran DL, Hoffmann B, Lussi A, Steinemann SG. Enhanced bone apposition to a chemically modified SLA titanium surface. J Dent Res 2004;83:529–533.
4. Hammerle C. Current issues forum. Int J Oral Maxillofac Implants 2005;20:311–312.
5. Puleo DA, Nanci A. Understanding and controlling the bone–implant interface. Biomaterials 1999;20:2311–2321.

6. Morra M, Cassinelli C, Cascardo G, Cahalan P, Cahalan L, Fini M, Giardino R. Surface engineering of titanium by collagen immobilization. Surface characterization and in vitro and in vivo studies. Biomaterials 2003;24:4639–4654.

7. Morra M, Cassinelli C, Meda L, Fini M, Giavaresi G, Giardino R. Surface analysis and effects on interfacial bone microhardness of collagen-coated titanium implants: A rabbit model. Int J Oral Maxillofac Implants 2005;20:23–30.

8. Morra M, Cassinelli C, Fini M, Giardino R. Enhanced osteointegration by biochemical surface modification: Covalent linking of collagen I to intervertebral metal disk surface. Eur Cells Mater 2005;10(suppl. 3):6.

9. Morra M, Cassinelli C, Cascardo G, Carpi A, Fini M, Giavaresi G, Giardino R. Adsorption of cationic antibacterial on collagen-coated titanium implant devices. Biomed Pharmacother 2004; 58:418–422.

10. Dunn DS, Raghavan S, Volz RG. Gentamicin sulfate attachment and release from anodized Ti-6Al-4V orthopedic materials. J Biomed Mater Res 1993;27:895–900.

11. Sul YT. The significance of the surface properties of oxidized titanium to the bone response: Special emphasis on potential biochemical bonding of oxidized titanium implant. Biomaterials 2003;24:3893–3907.

12. Li LH, Kong YM, Kim HW, Kim YW, Kim HE, Heo SJ, Koak JY. Improved biological performance of Ti implants due to surface modification by micro-arc oxidation. Biomaterials 2004;25:2867–2875.

13. Carinci F, Pezzetti F, Volinia S, Francioso F, Arcelli D, Marchesini J, Caramelli E, Piattelli A. Analysis of MG63 osteoblastic-cell response to a new nanoporous implant surface by means of a microarray technology. Clin Oral Implants Res 2004;15:180–186.

14. Davies JD. Understanding peri-implant endosseous healing. J Dent Ed 2003;67:932–949.

15. Cunningham BW. Basic scientific considerations in total disc arthroplasty, Spine J 2004;4:219S–230S.

16. Rickard DJ, Sullivan TA, Shenker BJ, Leboy PS, Kazhdan I. Induction of rapid osteoblast differentiation in rat bone marrow stromal cell cultures by dexamethasone and BMP-2. Dev Biol 1994;161:218–228.

17. Cheng SL, Yang JW, Rifas L, Zhang SF, Avioli LV. Differentiation of human bone marrow osteogenic stromal cells in vitro: Induction of the osteoblast phenotype by dexamethasone. Endocrinology 1994;134:277–286.

18. Ter Brugge PJ, Jansen JA. In vitro osteogenic differentiation of rat bone marrow cells subcultured with and without dexamethasone. Tissue Eng 2002;8:321–331.

19. Ohgushi H, Dohi Y, Yoshikawa T, Tamai S, Tabata S, Okunaga K, Shibuya T. Osteogenic differentiation of cultured marrow stromal stem cells on the surface of bioactive glass ceramics. J Biomed Mater Res 1996;32:341–348.

20. Dieudonne SC, van den Dolder J, de Ruijter JE, Paldan H, Peltola T, van't Hof MA, Happonen RP, Jansen JA. Osteoblast differentiation of bone marrow stromal cells cultured on silica gel and sol-gel-derived titania. Biomaterials 2002;23:3041–3051.

21. Minamide A, Yoshida M, Kawakami M, Yamasaki S, Kojima H, Hashizume H, Boden SD. The use of cultured bone marrow cells in type I collagen gel and porous hydroxyapatite for posterolateral lumbar spine fusion. Spine 2005;30:1134–1138.

22. Radin S, Reilly G, Bhargave G, Leboy PS, Ducheyne P. Osteogenic effects of bioactive glass on bone marrow stromal cells. J Biomed Mater Res A 2005;73:21–29.

23. Sul YT, Johansson C, Wennerberg A, Cho LR, Chang BS, Albrektsson T. Optimum surface properties of oxidized implants for reinforcement of osseointegration: surface chemistry, oxide thickness, porosity, roughness, and crystal structure. Int J Oral Maxillofac Implants 2005;20:349–359.

24. Yasuda H. Plasma Polymerization. Orlando: Academic Press; 1985.

25. Sul YT, Johansson CB, Petronis S, Krozer A, Jeong Y, Wennerberg A, Albrektsson T. Characteristics of the surface oxides on turned and electrochemically oxidized pure titanium implants up to dielectric breakdown: The oxide thickness, micropore configurations, surface roughness, crystal structure and chemical composition. Biomaterials 2002;23:491–501.

26. Morra M, Cassinelli C, Bruzzone G, Carpi A, Di Santi G, Giardino R, Fini M. Surface chemistry effects of topography modification of titanium dental implants surfaces. I. Surface analysis. Int J Oral Maxillofac Implants 2003;18:40–45.

27. Briggs D, Seah MP, editors. Practical Surface Analysis, 2nd ed. Chichester: Wiley; 1990. Vol. 1.

28. Sanden B, Olerud C, Johansson C, Larsson S. Improved bone-screw interface with hydroxyapatite coating. An in vivo study of loaded pedicle screws in sheep. Spine 2001;26:2673–2678.

29. Fini M, Giavaresi G, Greggi T, Martini L, Nicoli Aldini N, Parisini P, Giardino R. Biological assessment of the bone-screw interface after insertion of uncoated and hydroxyapatite-coated pedicular screws in osteopenic sheep. J Biomed Mater Res 2003;66:176–183.

30. Jansen JA, Vercaigne S, Hulshoff AG, Corten FGA, ter Brugge PJ, Naert I. The effect of surface roughness and calcium phosphate coating on bone regenerative impant surfaces. In: Davies JE, editor. Bone Engineering. Toronto, Em Squared; 2000. p 345–357.

31. Schliephake H, Scharnweber D, Dard M, Sewing A, Aref A, Roessler S. Functionalization of dental implant surfaces using adhesion molecules. J Biomed Mater Res B. Appl Biomater 2005;73:88–96.

32. Kim HW, Li LH, Lee EJ, Lee SH, Kim HE. Fibrillar assembly and stability of collagen coating on titanium for improved osteoblast responses. J Biomed Mater Res A 2005;75:629–638.

33. Davies JE, editor. Bone Engineering. Toronto: Em Squared; 2000. p 187.

34. Lebaron RG, Athanasiou KA. Extracellular matrix cell adhesion peptides: Functional applications in orthopedic materials. Tissue Eng 2000;6:85–104.

35. Mizuno M, Fujisawa R, Kuboki Y. Type I collagen-induced osteoblastic differentiation of bone-marrow cells mediated by collagen-$\alpha 2\beta 1$ integrin interaction. J Cell Physiol 200;184:207–213.

36. Jikko A, Harris SE, Chen D, Mendrick DL, Damsky CH. Collagen integrin receptors regulate early osteoblast differentiation induced by BMP-2. J Bone Miner Res 1999;14:1075–1083.

37. Salasznyk RM, Williams WA, Boskey A, Batorsky A, Plopper GE. Adhesion to vitronectin and collagen I promotes osteogenic differentiation of human mesenchymal stem cells. J Biomed Biotechnol 2004;1:24–34

38. Dardik R, Loscalzo J, Inbal A. Factor XIII (FXIII) and angiogenesis. J Thromb Haemost 2006;4:19–25.